Elucidation of the role of eccD3 in M. smegmatis

cell wall structure

5.1   Introduction

One of the unique features of bacteria is its cell wall chemistry and the complex architecture. The cell wall is of critical importance to the structure and the functioning of the organism. The cell wall composition and structure have a great significance in terms of the evolutionary success of some of the long persisting and still evolving pathogens like *M. tuberculosis*. The recent emergence of the MDR, XDR and TDR strains of *M. tuberculosis* is particularly alarming and calls for intensive investigation of the *M. tuberculosis* cell wall in order to gain a better understanding of the pathogenicity of these evolving strains.

While it is known that the lipid-rich thick cell wall allows the pathogen to withstand the actions of antibiotics and antimicrobial peptides, the bacterial factors and pathways regulating the composition of the cell wall are not completely understood. Thus, studies on basic pathways responsible for coordinated bacterial proliferation along with cell wall formation can provide critical insights into the survival mechanisms used by *M. tuberculosis*.

Through time immemorial bacteria evolved various shapes and sizes so as to survive in the diverse environmental conditions [1]. The shape of the bacterium influences a number of physiological adaptations such as nutrient acquisition, attachment, motility, polar and cellular differentiation [2]. The morphology of the bacterial cell is an important selectable trait and is largely controlled by the composition of the bacterial cell wall and the actin-like cytoskeleton [3]. The fate of the bacteria as far as its shape is concerned largely depends on the newly synthesized cell wall. Cell wall synthesis and cell division are both coordinated processes but are much less understood. The synthesis of the nascent cell wall contributes to maintaining the shape of the bacterium thus preserving the overall integrity which is of critical importance for cell viability. The *Mycobacterium sp.* has a unique cell wall having the characteristics of both Gram-positive and Gram-negative bacteria responsible for protecting itself from the external stress [4,5]. It has been reported that mutations resulting in defective cell shape of the bacteria are directly associated with defective cell wall synthesis machinery. The homolog of the DivIVA protein, Wag31 in *M. smegmatis* responsible for the regulation of localized cell wall synthesis is critical for maintaining the rod shape of mycobacteria [6]. The bacterial cytoskeleton actin homolog, MreB is also important for bacterial cell elongation and maintenance of a rod-like shape [7]. MreB was later reported to be directly or indirectly associated

with a number of proteins involved in cell-wall assembly, such that MreB was reported to regulate the cell-wall assembly machinery [8]. Deletion of RipA, a peptidoglycan endopeptidase responsible for the normal morphology of the mycobacteria, results in higher susceptibility of the bacterium towards antibiotics targeting the cell wall [9]. All these findings suggested that the precise composition of the cell wall is critical for maintaining the shape of the *Mycobacterium sp.*

The unique cell wall of the *Mycobacterium sp.* is critical for the physiology and survival of the bacterium as it performs several important functions such as protection from the hostile environment, imparting mechanical resistance to the cells, transport of the nutrients and the secreted proteins and lastly adhesion to target cells. The hallmark of mycobacterial cell wall is the presence of the thick waxy outer coat. Reports suggest that about 40% of the dry weight of the mycobacterial cell wall is composed of lipid [10,11]. In comparison to the 20% lipids present in other Gram positive bacteria, *Mycobacterium sp.* harbors almost 60% lipids. The mycobacterial lipids are typically composed of long chain fatty acids to which another layer of arabinogalactan is esterified and the arabinogalactan layer is attached to the peptidoglycan layer [4]. A number of important biological roles are attributed to the cell wall lipids such as maintaining low fluidity of the membrane thereby limiting the entry of non-recognizable compounds and resistance to the antibiotics [12,13]. Since this outer mycomembrane layer constitutes the major defense mechanism of the bacteria to survive in the hostile environment, the chemistry and biosynthesis of mycolic acids are of greater importance. With the emergence of multidrug-resistant and total drug resistant mycobacterial strains, the metabolic pathway of mycolic acid synthesis represents potential targets for the development of anti-tuberculosis drugs.

In mycobacterial species, the precursors of mycolic acid are synthesized by the two fatty acid synthases (FASs), the eukaryotic like FAS I and the bacterial like FAS II [14]. The multicomponent FAS I synthesizes the α branch [CH(R)COOH] consisting of C_{22-26} fatty acids and proceeds through five stages. The precursor molecule for the mycolic acid synthesis is the acetyl group. In the first stage the acetyl group is elongated by two carbon units and subsequently in the following stages fatty acids comprising of C_{20-26} are produced by the FAS I system [15] (Figure 5.1).
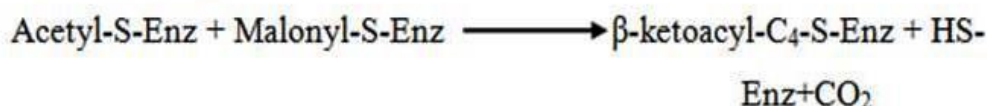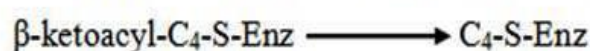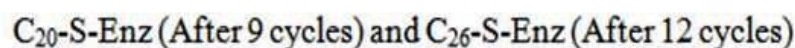
I.   **Acetyl transacylation**

Acetyl-CoA + HS-Enz $\longrightarrow$ Acetyl-S—Enz + CoA

II.   **Malonyl transacylation**

Malonyl-CoA + HS-Enz $\longrightarrow$ Malonyl-S-Enz + CoA

III. **Condensation**

Acetyl-S-Enz + Malonyl-S-Enz $\longrightarrow$ β-ketoacyl-C_4-S-Enz + HS-Enz+CO_2

IV.   **Sum of β-ketoacyl reduction, dehydration and enoyl reduction**

β-ketoacyl-C_4-S-Enz $\longrightarrow$ C_4-S-Enz

V.   **Recycling leads to two key products**

C_{20}-S-Enz (After 9 cycles) and C_{26}-S-Enz (After 12 cycles)

Figure 5.1: Reactions involved in the FAS I system in the formation of precursor fatty acid (C_{20}) for the FAS II system. Adapted from [15].

The fatty acid with C_{20} acts as the precursor molecule for the FAS II system. This is then followed by the elongation of the α branch by the very long meromyolic chains also known as the β-unit or straight portion [R-CH(OH)] by the dissociated FASII enzymes [15]. The elongation of the meromycolic chain is then accompanied by the introduction of two *cis* double bonds at the distal position of the mero chain. Till date, the exact mechanism for the incorporation of the double bond is not known. In this regard, three hypothesis are forwarded, (i) involvement of a dehydratase and invertase enzyme involved in the dehydration of b-hydroxydecanoyl-ACP to *trans* double bond and thereby isomerization to *cis* double bond; (ii) presence of a desaturase enzyme necessary for the addition of the double bond in the mycolic chain and (iii) the enzyme/s involved in the condensation reaction between the precursor fatty acids (C_{20}, C_{16}, and C_{22}) may result in the introduction of the double bonds. The presence of the *cis* double bonds in all the three component of mycolic acid is a remarkable and unique feature of the mycobacterial cell wall.

Mycobacterial cell wall mycolic acid comprises of structurally related molecules that differ in the number of carbon atoms and functional groups at the distal and proximal positions. The least polar mycolic acid is the α mycolic acid which consists of C_{76-82} in *M. tuberculosis* and *M. bovis* with two *cis*-cyclopropyl groups

[16,17]. In the fast growing non-pathogenic *Mycobacterium sp., M. smegmatis*, two *cis* double bonds are present instead of the cyclopropyl groups [18]. The cyclopropanation of the α mycolic acid in *M. tuberculosis* and *M. bovis* plays a pivotal role in virulence [19]. The cyclopropanation of the α mycolic acid affects the membrane function either by imparting membrane rigidity or by providing resistance to oxidative stress [20,21]. The second type of mycolic acid known as the α′ mycolic acid is composed of fatty acid comprising of C_{60-62} with one *cis* double bond. The third type of mycolic acid contains a supplementary oxygen function present in the distal position of the meromycolic chain and is known as keto-, methoxy-, and hydroxyl- in case of *M. tuberculosis* and epoxy-, in the non-pathogenic strain *M. smegmatis* [22]. The chain lengths of the methoxy-, keto-, and hydroxy- mycolic acids in *M. tuberculosis* ranges from C_{84-88} whereas, in the non-tuberculous mycobacteria, the epoxy-mycolic acid have a chain length comprising of the same number of carbon atom present in the α mycolic acid of the same species (Figure 5.2, 5.3) [16, 23].
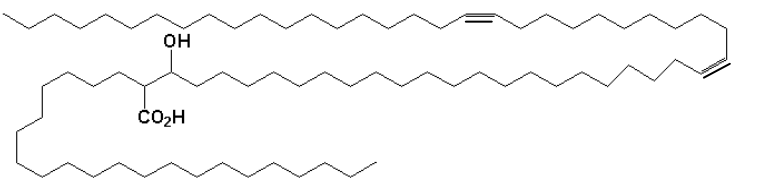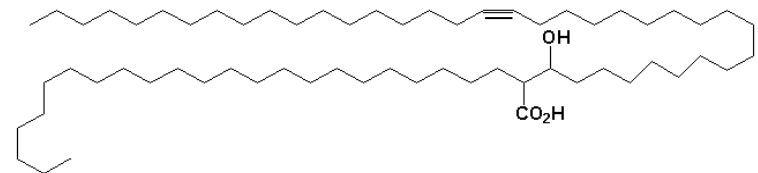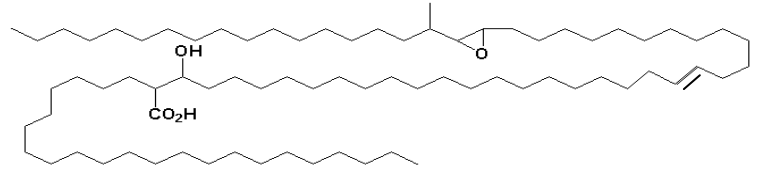
Type of mycolate	Mero chain structure
α *cis*	
α'	
Epoxy	

Figure 5.2: Mycolic acid subspecies of *M. smegmatis* [16]
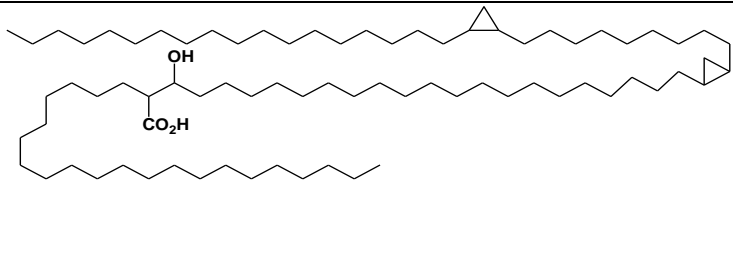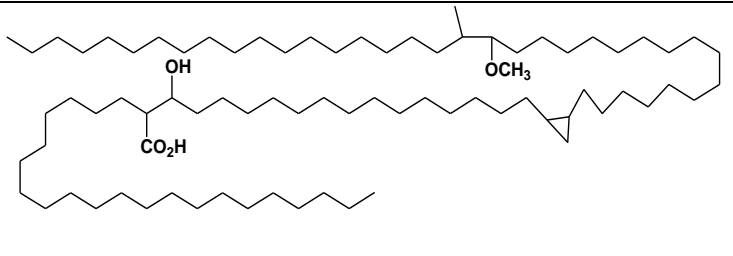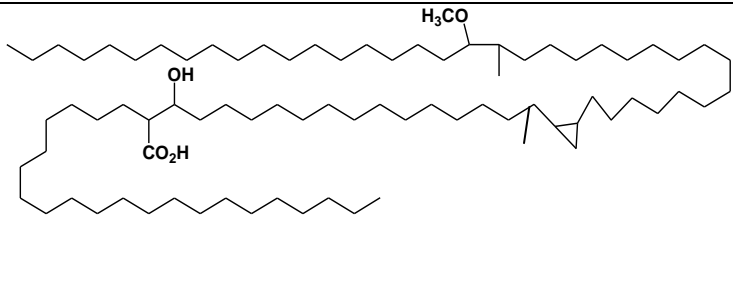
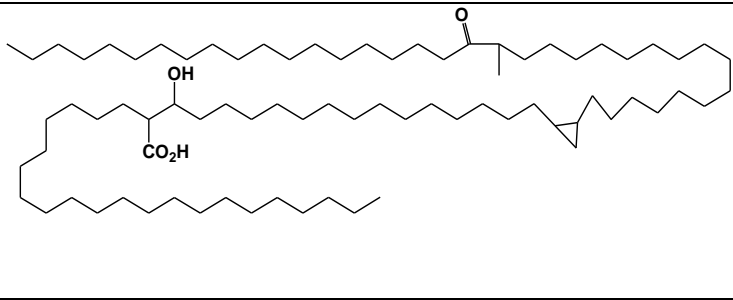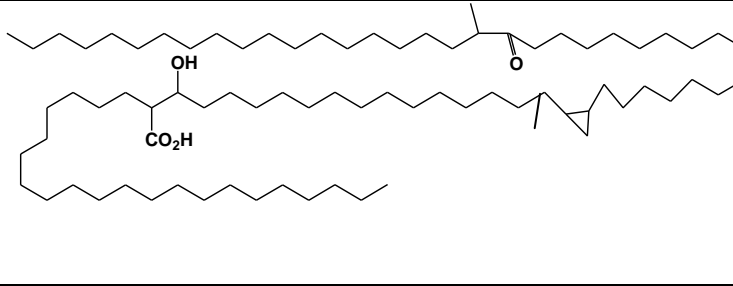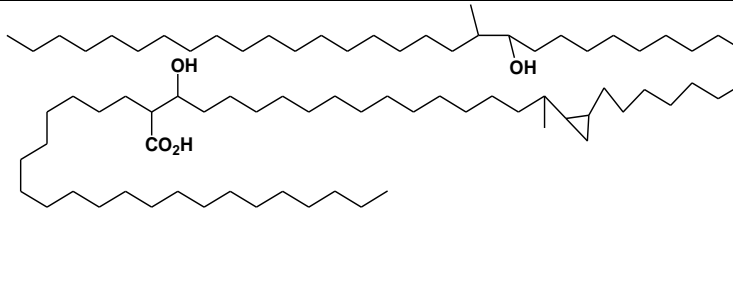| Type of mycolate	Mero chain structure
cis	
Methoxy *cis*	
Methoxy *trans*	
Keto- *cis*	
Keto *trans*	
Hydroxyl *trans*	

Figure 5.3: Mycolic acid subspecies of *M. tuberculosis* [23]

Mycobacterium sp. exchanges materials across its thick lipid-rich highly impermeable membrane essential for its survival through the different secretory apparatus. One such unique secretory apparatus is the Type VII secretion system (T7SS), conserved among all *Mycobacterium sp*. [24]. There are five clusters of T7SS designated as ESX-1, ESX-2, ESX-3, ESX-4 and ESX-5 [25]. Out of the five T7SS clusters, the ESX3 is one of the most widely conserved systems among the entire mycobacterial sp that help the mycobacteria in the metal iron homeostasis [26,27]. Although *Mycobacterium sp.* is known to have five different ESX loci, the fast-growing *Mycobacterium sp.* has a less number of ESX secretion systems. The fast-growing nonpathogenic strain *M. smegmatis* has three of such ESX loci homologs, ESX-1, ESX-3, and ESX-4 [25]. The ESX-1 secrets the ESAT-6 and CFP10 proteins similar to the pathogenic species while the ESX-3 helps in the normal growth of the bacteria by the regulated sequestration of iron. The five T7SS, in general, comprises of five ESX conserved components (Ecc) christened as EccA, EccB, EccC, EccD and EccE. The core components of the T7SS are EccB, EccC, EccD, and EccE that form the inner channel in the membrane. The role of EccB and EccE in the secretory apparatus is not very clear while the EccC functions as a coupling component and provides energy in the transfer of protein across the mycobacterial membrane while EccD forms the central channel of the secretory apparatus in the mycobacterial membrane. It has been reported that, disruption of the core component; EccD5 of the ESX-5 loci abolishes the stability of the secretory apparatus which is involved in maintaining the cell wall integrity of the bacterium. The EccD3 of the ESX-3 secretion system also helps in maintaining the permeability and integrity of the mycobacterial cell wall as has been discussed in the previous chapter. Apart from these studies, there are limited number of reports of how these components of the secretory apparatus control the permeability and integrity of the mycobacterial cell wall thus playing a significant role in the maintenance of the bacterial shape. *M. smegmatis* has a conserved ESX-3 secretory apparatus in which the EccD3 forms the central channel of the secretory apparatus. In our previous chapter, EccD3 is reported to be important for *in vitro* growth and maintenance of the cell wall integrity. The present chapter describes the study on the role of the EccD3 in maintaining the composition of the cell wall which influences the shape and size of the mycobacteria.

5.2   Materials and methods

5.2.1   *Bacteria strain, plasmid, and growth conditions*

The wild-type *M. smegmatis* mc^{2}155 and the *eccD3* deleted *M. smegmatis* mutant, Ms0622 were grown in Middlebrook 7H9 (MB-7H9) medium supplemented with 0.05% Tween80 and 0.2% glycerol or Middlebrook 7H10 (MB7H10) plates supplemented with 0.5% glycerol. The antibiotics were added in the following concentrations, Kanamycin (25μg/ml for *M. smegmatis*) and hygromycin (10μg/ml for the mutant strain). Both the wild-type and the mutant strains were grown at 37°C for 16 hours.

5.2.2   *Confocal Laser Scanning Microscopy*

Wild-type *M. smegmatis* (mc^{2}155) and the mutant strain (Ms0622) were grown in MB-7H9 media (supplemented with .5% glycerol and 0.05% Tween80) at pH 6.8. The cells were pelleted and washed with PBS three times. The pellets thus obtained were stained with DAPI (2μg/mL in H_2O, stock solution; Invitrogen D1306) for 10 mins. Smears of both the wild-type and the mutant strains were prepared in glass slides. The slides were fixed using 3.7% formaldehyde for 10 mins at room temperature. The cells were mounted on the confocal microscope (Olympus 1X81) for imaging.

5.2.3   *Scanning electron microscopy (SEM)*

Samples were prepared for SEM with slight modifications [28]. Briefly, bacteria were grown to an OD_{600} of 0.6 and resuspended in 10mM sodium phosphate buffer, pH 7. The bacteria were then washed and fixed overnight with 2.5% (v/v) glutaraldehyde (Sigma). The cells were mounted on coverslips using poly (L-lysine) and rinsed with 10mM sodium phosphate buffer, pH 7.4. The coverslips were dehydrated through an ethanol series 30%, 50%, 75%, 90% and 2 x 100%, 5 mins each. The samples were dried at 37^{0}C and coated with 10–15nm thickness of gold/palladium (60:40) alloy using a BAL-TEC SCD-005 sputter coater. Samples were examined using a JEOL 5600 LV scanning electron microscope with an accelerating voltage of 10 kV.

5.2.4   *Extraction of mycobacterial mycolic acids*

Mycolic acid was extracted from *M. smegmatis* as described [29]. Briefly, the wild-type and the mutant strains were inoculated in MB-7H9 broth and incubated at

37^0C such that the OD_{600} is 0.8-1.0. The cells were harvested by centrifugation at 3,000 rpm for 10 mins at room temperature. The pellet was washed with 5ml of water. It was then transferred to a glass tube prior to the hydrolysis of lipid. The bacterial pellet was suspended in 2ml of tetrabutylammonium hydroxide (TBAH) and incubated overnight at 100^0C using a heating block. The tube was allowed to cool down and the fatty/mycolic acids were methyl esterified. To the TBAH mixture, CH_2Cl_2 (4 ml), CH3I (300µl) and water (2ml) was added. The tube was mixed on a rotator for 1 hour and centrifuged at 3,500 rpm for 10 mins at room temperature. This allowed separation of the mixture in two phases: a lower organic phase containing the lipids and an upper aqueous phase. The upper phase was discarded. 4ml of water was added and spun at 3,500 rpm for 10 mins at room temperature. The washing was repeated twice and the upper phase was discarded. The lower organic phase was dried and 3ml diethyl ether was added and sonicated in a water bath for 10 mins. It was then followed by another round of centrifugation at 3,500 rpm for 10 mins at room temperature. The fatty acid/mycolic acid methyl esters were transferred to a glass tube using a Pasteur pipette. The diethyl ether was evaporated and the residue was resuspended in 100-200µl CH_2Cl_2.

5.2.5 Thin layer chromatography (TLC)

10-30µl of the extracted mycolic acid was spotted on an aluminum TLC plate using 10µl capillary tubes. The solvent system, hexane/ethyl acetate (19:1, v/v) was used for the separation of Fatty acid methyl esters (FAMES) and mycolic acid methyl esters (MAMES) by thin layer chromatography in a TLC chamber. The fatty acid mixture was spotted on the TLC plate and the plate was placed in the tank. This procedure was repeated twice to allow better separation. The TLC plates were sprayed with 5% ethanolic molybdophosphoric acid in a TLC spray cabinet. When the plates were charred, the constituting lipid subspecies were revealed.

5.2.6 Purification of the mycolic acid subspecies

MAMES were loaded on preparative TLC plates and separated, as described above. The subspecies of mycolic acid were visualized by spraying the plate with 0.01% ethanolic Rhodamine 6G. The individual mycolic acid subspecies were scraped off the plates and loaded into a glass tube. The individual mycolic acids were then eluted using diethyl ether. The solvent was evaporated and the purified mycolic acid subspecies were resuspended in 100-200µl CH_2Cl_2.

5.2.7 Differential Scanning Calorimetry (DSC)

DSC (SHIMADZU, DSC-60) was performed as described [21]. The purified individual mycolic acid subspecies along with 0.2ml of phosphate buffered saline was added to a crucible and subjected to a heating and cooling cycle at the rate of 30^0C/h in a range of 10 to 60^0C.

5.2.8 Gas Chromatography-Mass Spectrometry of MAMES

The derivatized trimethylsilylated subclasses of each mycolates were analyzed by GC/MS (Agilent Technologies, 7890A) fitted with DB5-MS DG column (30 m length, 0.25 mm inner diameter, 250 µm film thickness), over a programmed temperature range of 70°C, 295°C and 320°C for respective time intervals of 1, 12.5 and 25 mins, using an ion source of 70eV at 250^0C.

5.2.9 NMR Analysis of MAMES

^{1}H NMR spectra of methylated esters of both wild and mutant type mycolic acid subclasses were recorded on a 500mHz Bruker Advance NMR spectrophotometer using $CDCl_3$ solvent and trimethylsilane as the internal standard [31].

5.3   Results

5.3.1 Deletion of eccD3 leads to conversion of mycobacterial rods to coccus

The deletion of the *eccD3* gene belonging to the ESX3 T7SS resulted in the transformation of the rod-shaped mycobacteria to a spherical shape (Figure 5.4). When the nucleoid morphology was examined using fluorescence microscopy, *eccD3* deleted *M. smegmatis*, Ms0622 cells displayed differences in terms of normal size and shape. The size of the mutant cell was reduced to 2µm as compared to the wild-type which is 5µm. The DAPI-stained nucleoids were more diffused and spread throughout the cell in the *eccD3* deleted strain than the control cells, which had compact nucleoids.

Scanning electron microscopy (SEM) was used to analyze and compare the cell size and shape of the wild-type, mutant and the *eccD3* complemented *M. smegmatis* strains. SEM examination of the *eccD3* deleted mutant strain; Ms0622 indicated definite morphological changes that might be attributed to the deletion of the *eccD3* gene. The morphology of the *eccD3* deleted *M. smegmatis* cells seemed to have a tendency to converse itself from elongated rod shape to spherical shape (Figure

5.5). The size of the cells in the mutant strain was reduced by 4 fold in comparison to the wild-type cells. Complementation of the *eccD3* mutant showed that the cells have restored its rod shape and the size of the bacteria was comparable to the wild-type cells.
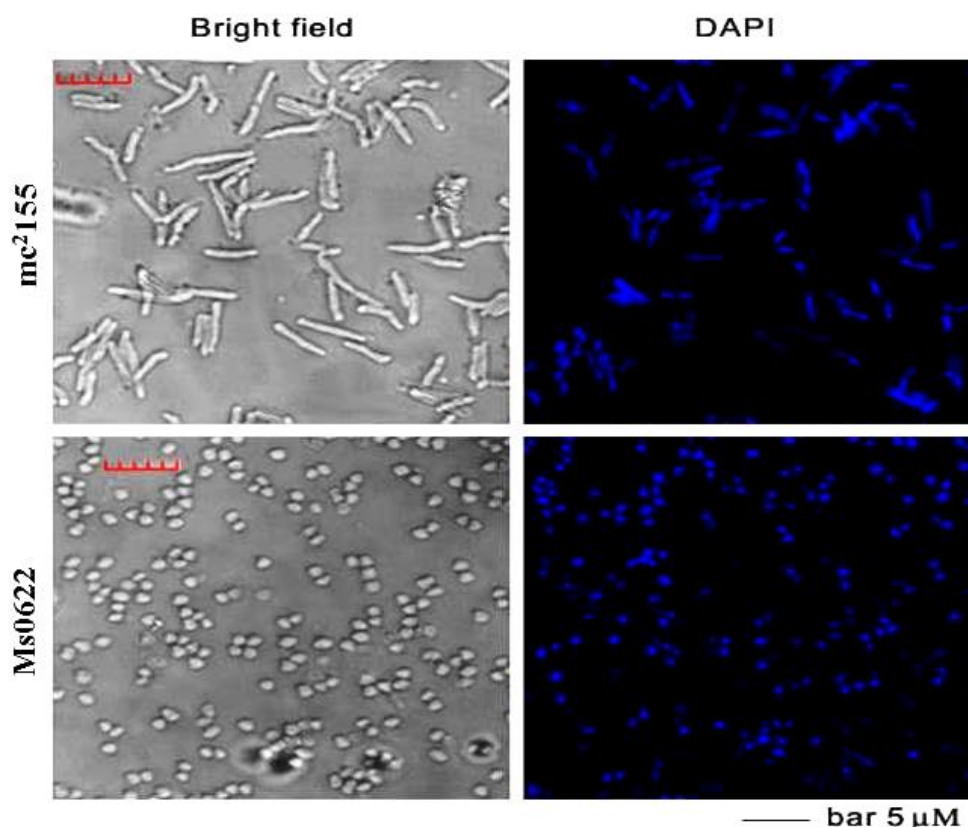

Figure 5.4: Confocal microscopy of the wild-type mc²155 and the *eccD3* deleted strain, Ms0622 of *M. smegmatis*.
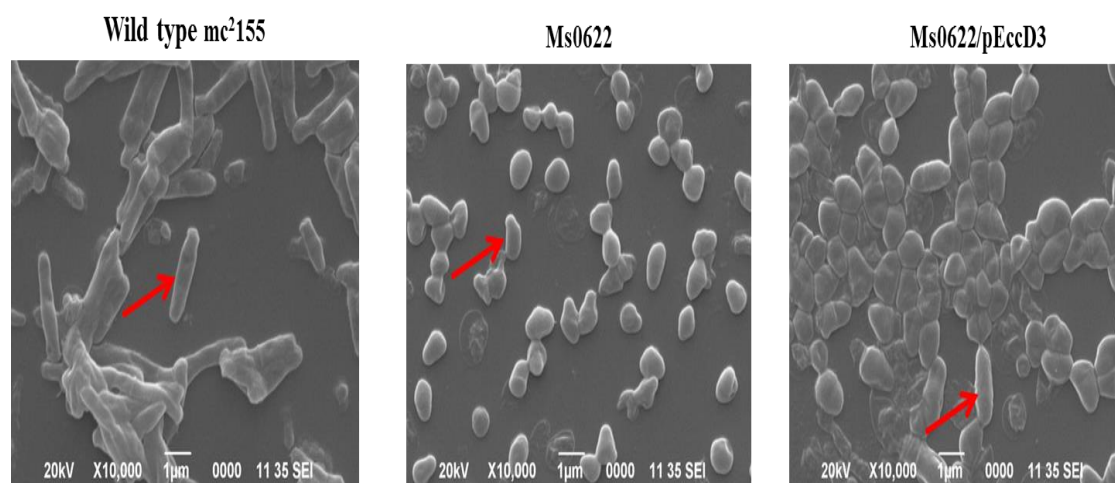

Figure 5.5: Scanning electron micrographs of the wild-type, mc²155; mutant Ms0622, and complemented strain, Ms0622/pEccD3 showing conversion of the rod shaped cells to irregular spherical cells upon deletion of *eccD3* in *M. smegmatis*.

5.3.2 Cell wall lipid analysis

The changes in colony morphology and biofilm formation reported in the previous chapter and the conversion of the rod-shaped bacillus to coccoid form suggested that deletion of *eccD3* affected some components of the mycobacterial cell wall. Since the mutation in the cell wall biosynthetic pathway affects the shape and colony morphology of the mycobacteria [32, 33], the deletion of *eccD3* prompted to examine the composition of mycolic acid in the mutant strain. A standard procedure for release of mycolic acids from mycobacteria involves base hydrolysis of cells with tetrabutylammonium hydroxide (TBAH). This is followed by the addition of Methyl iodide, which acts as a phase transfer catalyst and results in the formation of mycolic acid methyl esters (MAMEs) which are then analyzed by thin-layer chromatography (TLC) [34]. The individual mycolic acid subspecies were identified as specific bands on the TLC plates by comparing with related studies performed earlier [35]. While the parental strain showed the α, α′ and epoxy components of the mycolic acid methyl esters, the *eccD3* deleted strain was completely deficient of the α′ and epoxy components while the presence of the α component was comparatively less than the wild-type *M. smegmatis* (Figure 5.6). The absence of the α′ and epoxy components and relatively less amount of the α component of MAMEs in the *eccD3* deleted strain *vis-a-vis* the wild type, was indicative of the fact that *eccD3* is involved in the precise organization of the mycomembrane thus playing a pivotal role in the lipid biosynthesis pathway of *M. smegmatis*.
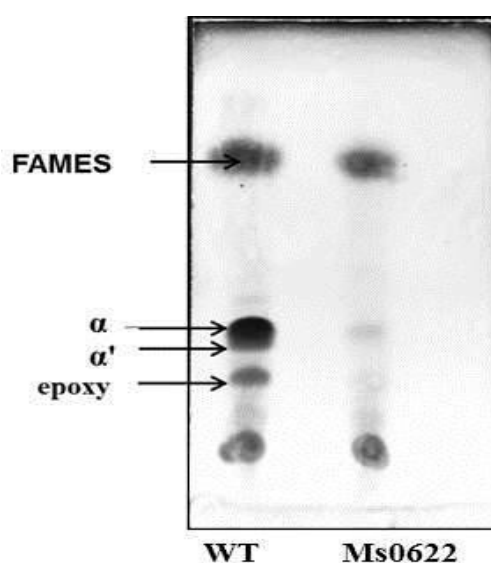

Figure 5.6: TLC analysis of Mycolic acid and Fatty acid methyl esters (MAMES and FAMES) of the wild type mc^{2}155 and the *eccD3* deleted strain, Ms0622 of *M. smegmatis*.

5.3.3 Effect of eccD3 deletion on Cell Wall Fluidity

The outer mycomembrane present in the cell wall of *Mycobacterium* contributes to the fluidity of its membrane thus conferring low permeability to the cell wall which in turn helps the bacteria to protect it from the obnoxious compounds [36]. The absence of the α′ and epoxy components of MAMES in the *eccD3* deleted strain might have altered the permeability of the cell wall. To assess the relative contributions of these modifications on the cell wall fluidity, both the purified methyl mycolic acids and the purified *M. smegmatis* cell wall from the parental and the mutant strain were examined by DSC. DSC scanning of the purified cell wall fraction from the wild-type strain, mc^{2}155 isolated after treatment with PMSF and Triton X-114 showed distinct thermal transitions at 31 ^{0}C and 80 ^{0}C. While, the purified cell wall fraction from the *eccD3* deleted strain, Ms0622 showed a single thermal transition at 42 ^{0}C (Figure 5.7 [A]). The reversibility of thermal transitions was confirmed by repeating the scanning cycle for four times. Purified MAMEs from the wild-type strain showed thermal transition at 31 ^{0}C whereas DSC scanning of the purified MAMES isolated from the *eccD3* deleted strain showed an increase in thermal transition at 37 ^{0}C (Figure 5.7 [B]).
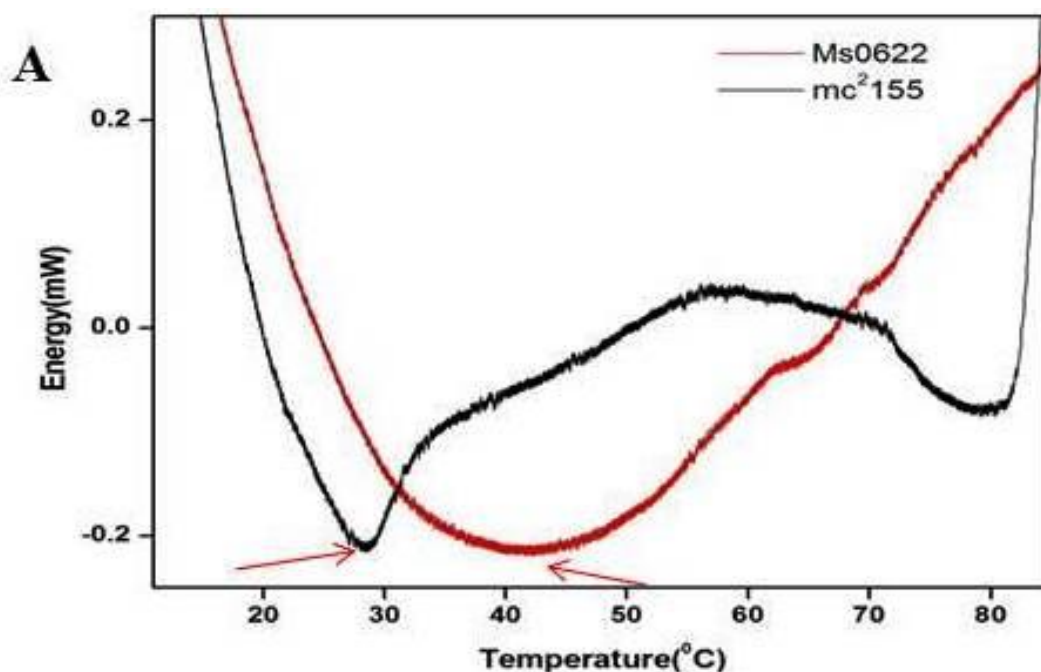

Figure 5.7 [A]: Differential scanning calorimetry of cell wall from Wild type *M. smegmatis* mc^{2}155, and *eccD3* deleted strain, Ms0622.
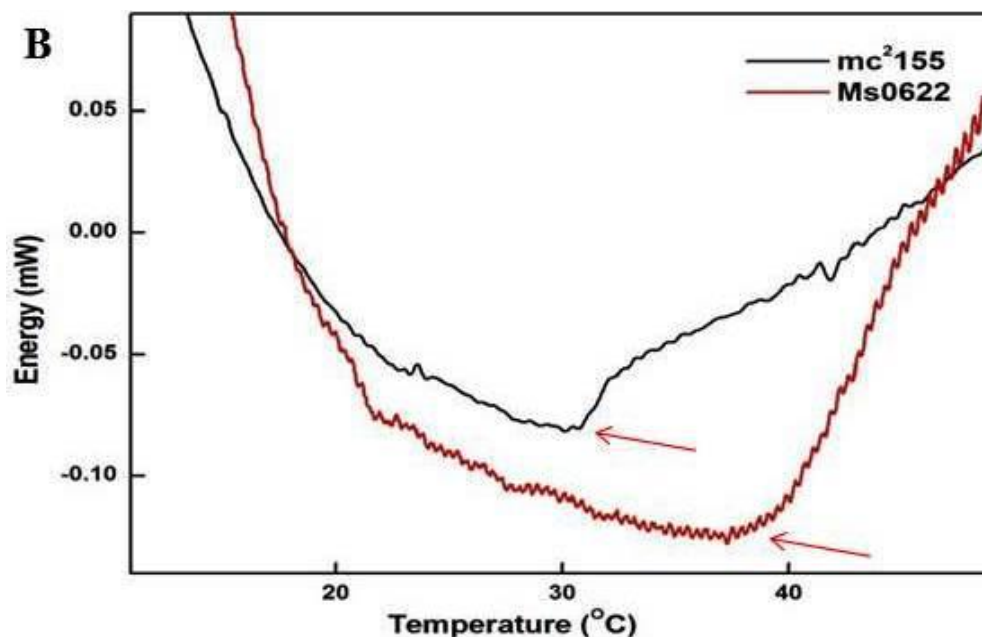
Figure 5.7 [B]: Differential scanning calorimetry of purified mycolic acids from Wild type *M. smegmatis* mc²155, and *eccD3* deleted strain, Ms0622.

5.3.4 Gas chromatographic/mass spectrometric analysis

The increase in the thermal transition temperature of the purified MAMEs and cell wall fractions from the mutant strain, Ms0622 was emblematic of the fact that the length and degree of unsaturation of the hydrocarbon tails of the individual subspecies of mycolic acid have been transformed. To examine this characteristic change, each subclass of these mycolic acid methyl esters was isolated, converted to its TMS derivative and analyzed by gas chromatography. The GC-MS analysis showed a mark difference in the *eccD3* deleted mutant as compared to the wild-type. The profiles of gas chromatograms of TMS derivatives of the non-polar fatty acid methyl esters (FAMES) recovered from the uppermost spot on TLC from the wild-type and the *eccD3* deleted mutant exhibited a number of significant peaks (Figure 5.8 [A], [B]). Both the parental and the mutant strain contained the major constitutive fatty acids and did not exhibit any major differences in the gas chromatogram.
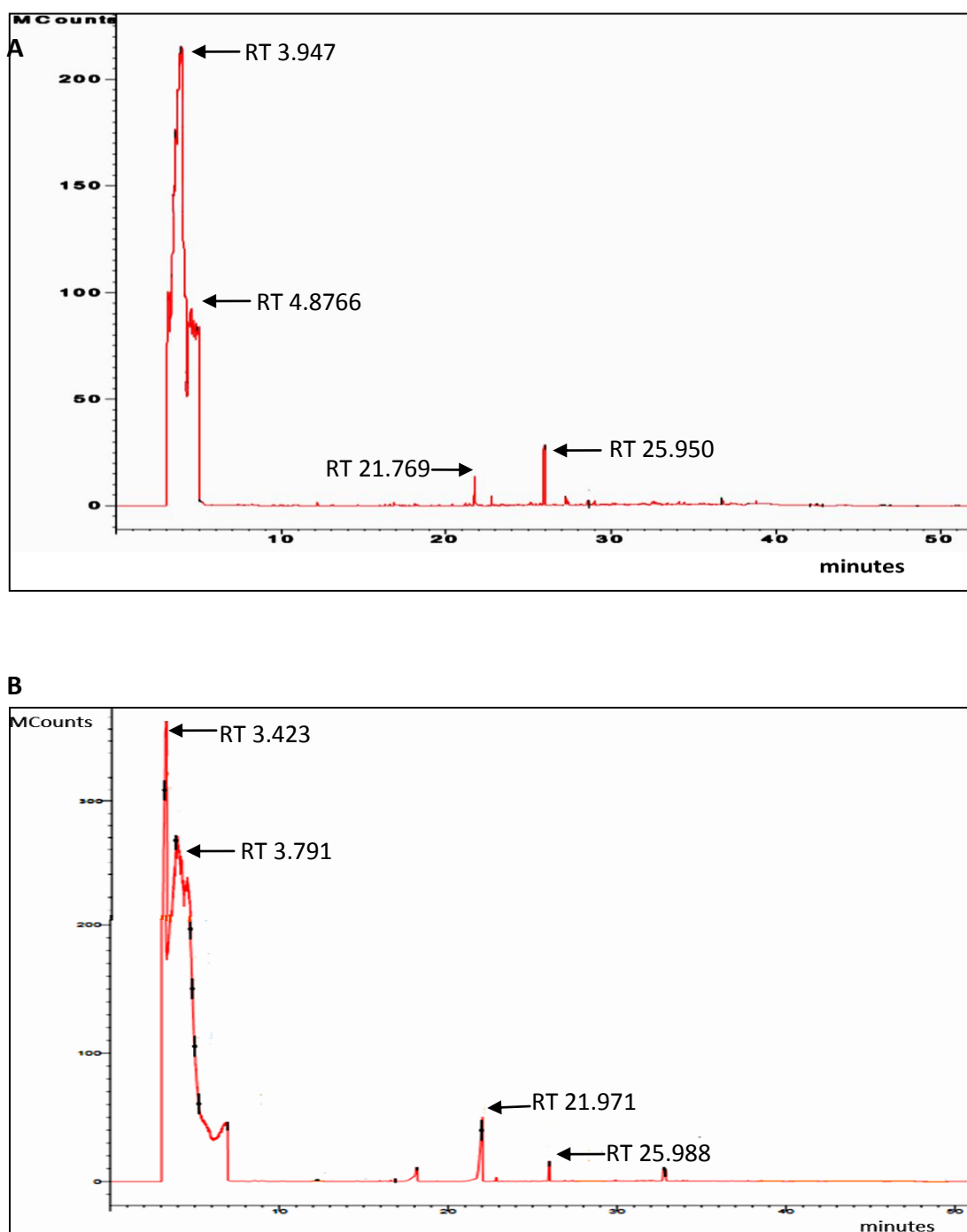
Figure 5.8: GC of the isolated FAMES from the (A) wild type *M. smegmatis* mc²155 and (B) deleted *M. smegmatis*, Ms0622.

The pyrolytic cleavage of the full-length mycolic acid methyl esters yields two major products, a short-chain saturated hexacosanoic acid and the long-chain meroaldehyde [37]. Pyrolytic cleavage of full-length mycolate has been described previously and was used in the initial structural characterization of these molecules [38,39,40]. The pyrolytic cleavage of C_2 and C_3 results into alpha unit or the branched chain structure while C_3-C_4 cleavage results into a long carboxylic acid ester ion that

carries a silane group [B$^+$] (Figure 5.9) [41,42]. In this study, [CH(R)COOH], the α unit or branched-chain structure corresponding to C_{22}, C_{24}, and C_{26} was monitored.
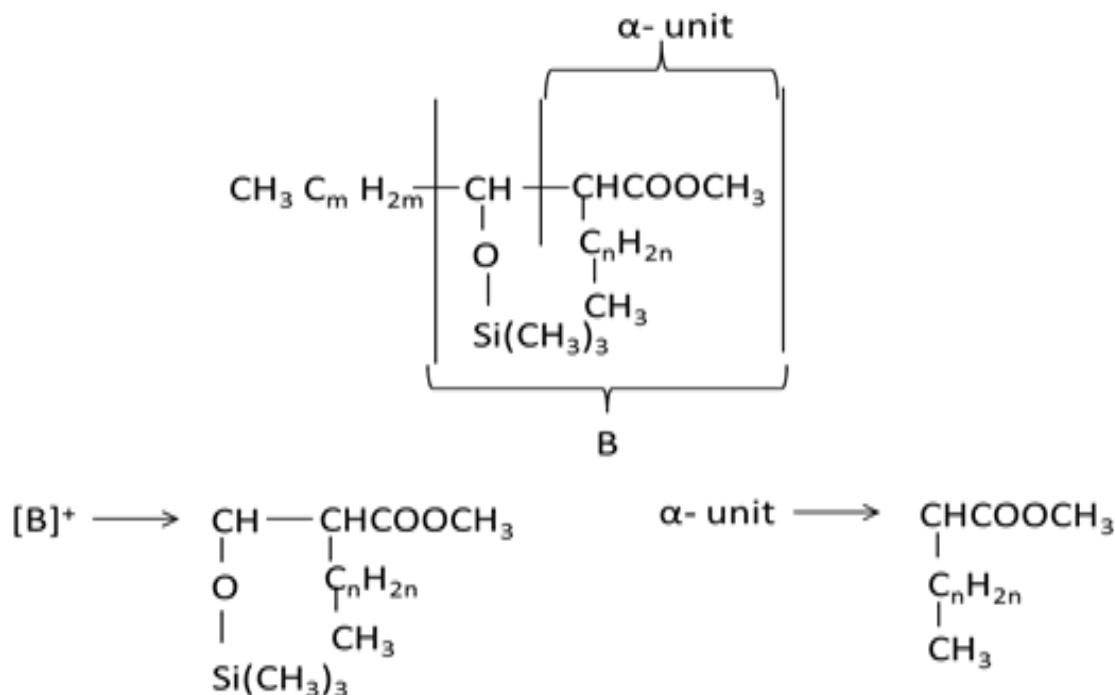

Figure 5.9: Pyrolytic cleavage of TMS derivatized mycolic acid methyl esters at C_3-C_4 and C_2-C_3 atom yields [B]$^+$ ion and the α-unit.

Pyrolysis GC analysis of α mycolic acid methyl esters isolated from the wild-type revealed peaks of C_{18}, C_{22} and C_{26} methyl esters corresponding to the α-unit at retention time 11.625 mins and 16.865 mins (Figure 5.10), while the GC of α mycolic acid methyl esters isolated from the mutant strain lacked the characteristic peaks at 11.625 mins and 16.865 mins instead the gas chromatogram of the mutant strain showed a peak at retention time 9.406 mins similar to the wild type (Figure 5.12). The peak area of $C_{22:0}$, and $C_{26:0}$ fatty acids present in the α component on gas chromatograms were measured and the percentage of each fatty acid [= $C_{22:0}$ or $C_{26:0}$/ ($C_{22:0}$ + $C_{26:0}$) * 100] was calculated [43]. While the α-unit of the parental strain of *M. smegmatis* consisted of 60% of $C_{22:1}$ and 39.9% $C_{26:1}$ in the α mycolic acid subspecies (Figure 5.11 [A], [B]), the carbon numbers of the α-unit of the *eccD3* deleted strain was seen to be decreased to C_{18} (Figure 5.13). Moreover, the α-unit in the wild-type contained a double bond whereas the *eccD3* deleted strain did not have any double bond.
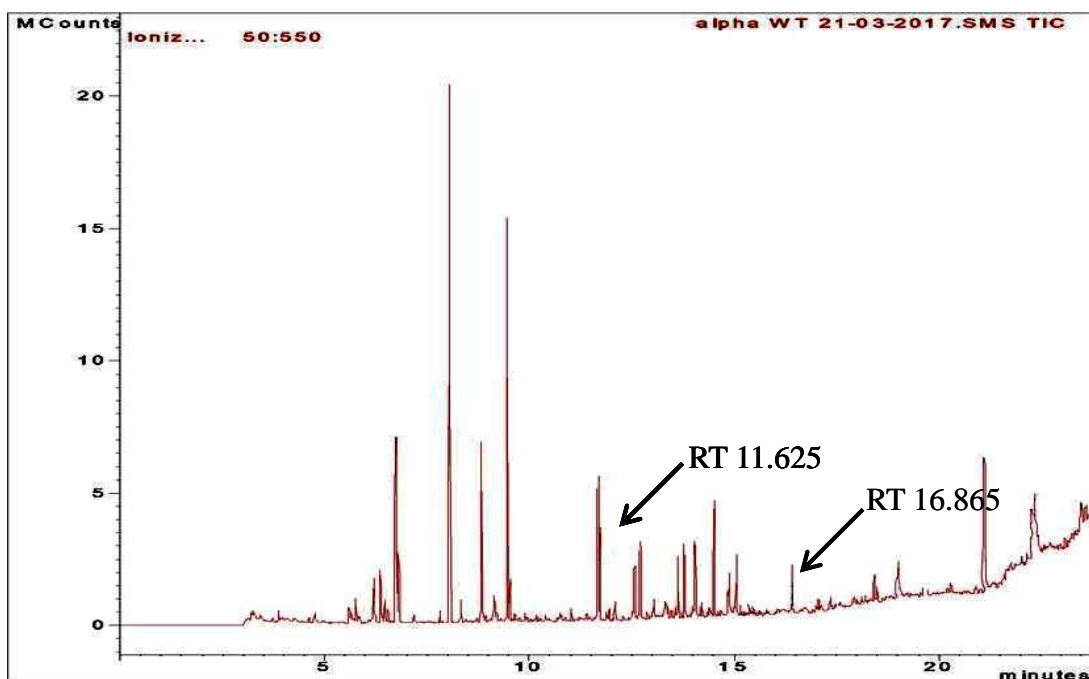
Figure 5.10: GC of the isolated α subspecies of mycolic acid methyl ester from the wild type *M. smegmatis* mc^{2}155.

A

B

MW: 340 C22H44O2 (mainlib) Heneicosanoic acid, methyl ester
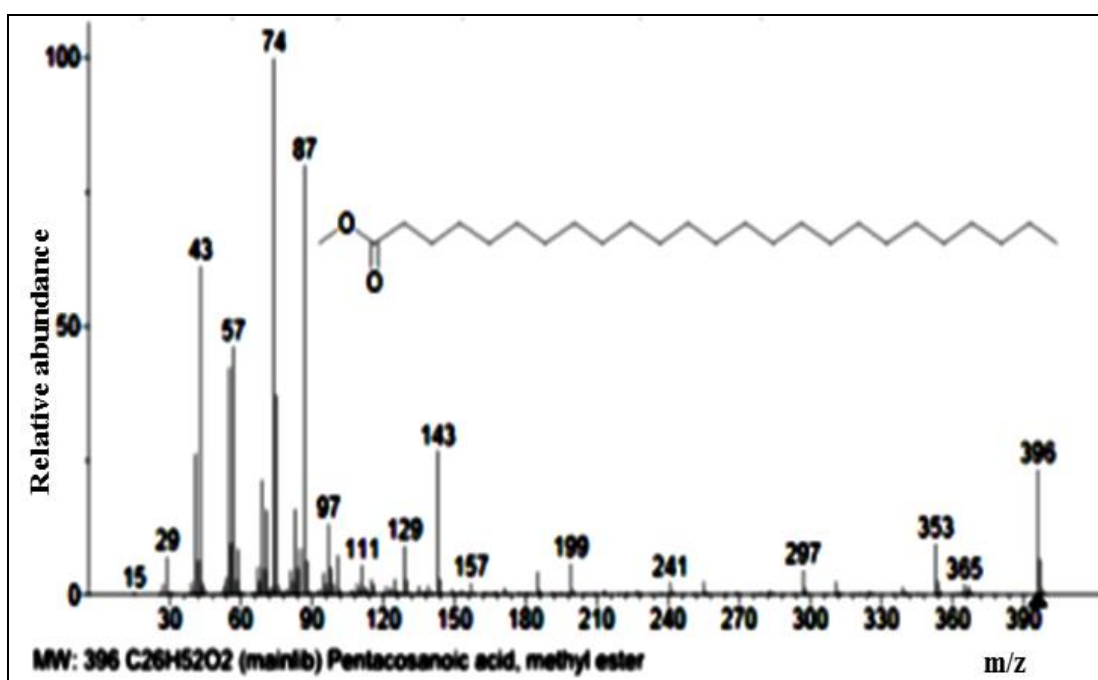
Figure 5.11: Mass spectra of trimethylsilyl ether derivatives of α-unit of the isolated α subspecies of mycolic acid methyl esters from the wild type *M. smegmatis* mc²155 at retention time [A] 11.625 mins and [B] 16.865 mins.
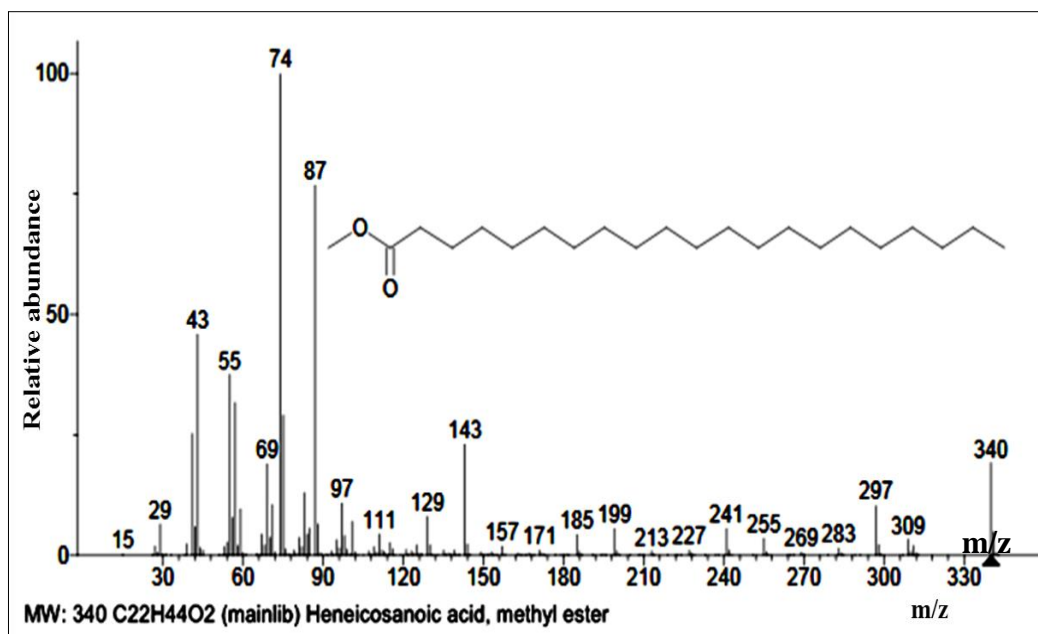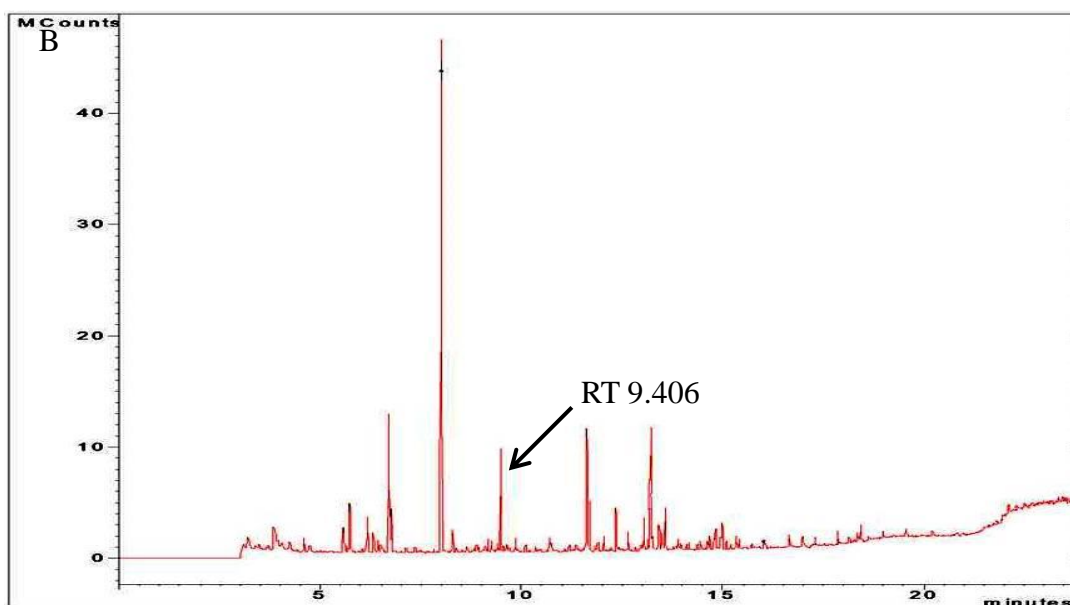

RT 9.406

Figure 5.12: GC of the isolated α subspecies of mycolic acid from the *eccD3* deleted *M. smegmatis*, Ms0622.
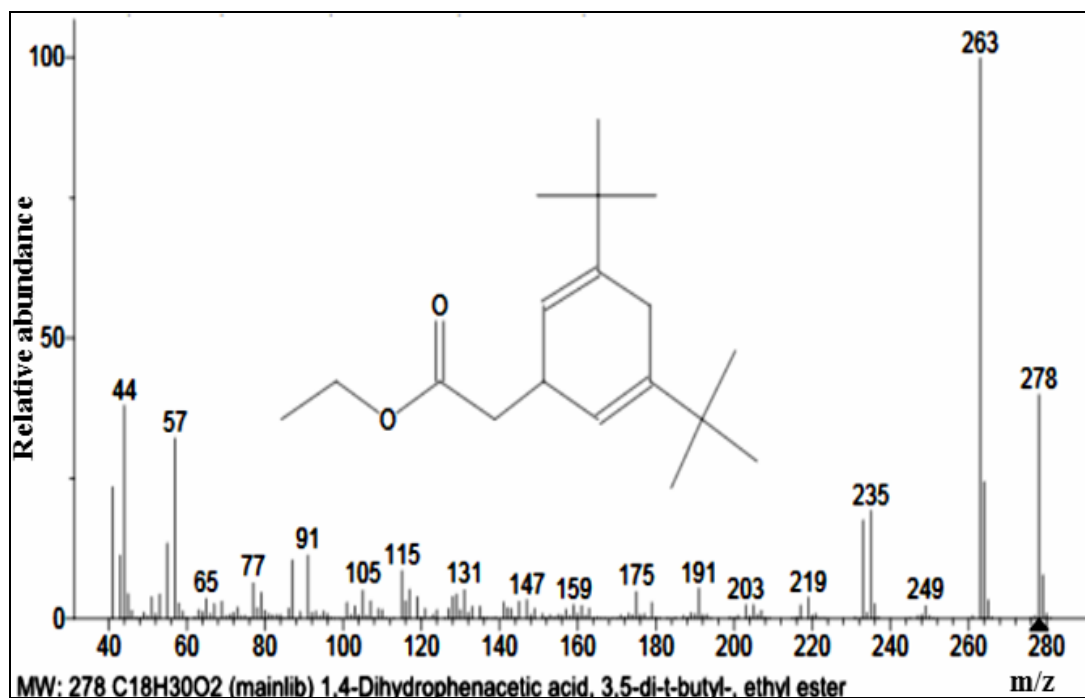
Figure 5.13: Mass spectra of trimethylsilyl ether derivatives of α-unit of the isolated α subspecies of mycolic acid from the *eccD3* deleted *M. smegmatis*, Ms0622 at retention time 9.406 mins.

5.3.5 NMR analysis

The methylated mycolic acid esters of each subspecies were examined by ^{1}H NMR spectroscopy. The α-mycolic acid of the parental strain, mc[2]155 exhibited several resonances in addition to the water signal at δ1.55 ppm and the CHCl$_3$ solvent signal at δ (ppm)=7.23 (Figure 5.14 [A]). The resonance peaks were assigned according to the reports described earlier [44,45]. Analysis of the α mycolic acid methyl ester from the parental strain by ^{1}H NMR revealed that the spectra contained signals due to terminal methyl groups at δ (ppm)=0.87 ([(CH$_2$)$_n$CH$_3$],triplet); intense signal at δ (ppm)=1.25 characteristic of the isolated methylene proton resonance [CH$_2$(CH$_2$)$_n$CH$_2$, broad singlet]. Besides the terminal and methylene protons, the α component also resonated at δ (ppm)= 1.56 [CH$_2$CH(OH), multiplet] and δ (ppm) =2.41 corresponding to the methine group. The characteristic peaks at δ (ppm)=2.17 and δ (ppm)=5.35 confirmed the presence of unsaturation in the α component of the mycolic acid methyl esters of the wild type strain. The peak at δ (ppm)=2.17(4H) was attributed to the protons of two methylene groups contiguous to the *cis* double bond (CH=CHCH$_n$ group, broad multiplet), while the resonance peak at δ (ppm)=5.35(2H, t) was attributed to the *cis*-double bond protons (-CH=CH-). The two double bonds

were observed to be in *cis* configuration as the resonance at δ (ppm)=5.35 appeared as a triplet of doublets with very less coupling constant (J=4.7). In addition, the absence of the characteristic resonance peak at δ (ppm)=0.95 of the α-methyl protons adjacent to the *trans* double bonds in mycolic acids confirmed the *cis-cis* conformation of the methylated mycolic acid ester double bonds. Furthermore, the NMR spectra also contained signals for protons of methoxyl group from the carboxyl methyl ester at δ (ppm)=3.71 (CHOH, singlet) and protons from methine at δ (ppm)=2.43, [CH(CO$_2$Me) multiplet)]. Whereas the ^{1}H NMR of the α component of the mycolic acid methyl ester from the mutant strain, Ms0622 exhibited a marked difference in the spectra (Figure 5.14 [B]). Although the ^{1}H NMR spectra of the *eccD3* deleted strain contained the assigned peaks for the terminal methyl group protons, methylene protons and methoxyl group protons from the carboxyl methyl ester, the signal for the protons adjacent to the *cis* double bond at δ (ppm)=5.35 was absent. The resonance peak at δ (ppm)=2.41 present in the wild type *M. smegmatis*, characteristic of the protons of the methine group was also absent in the *eccD3* deleted *M. smegmatis* strain.

A

B
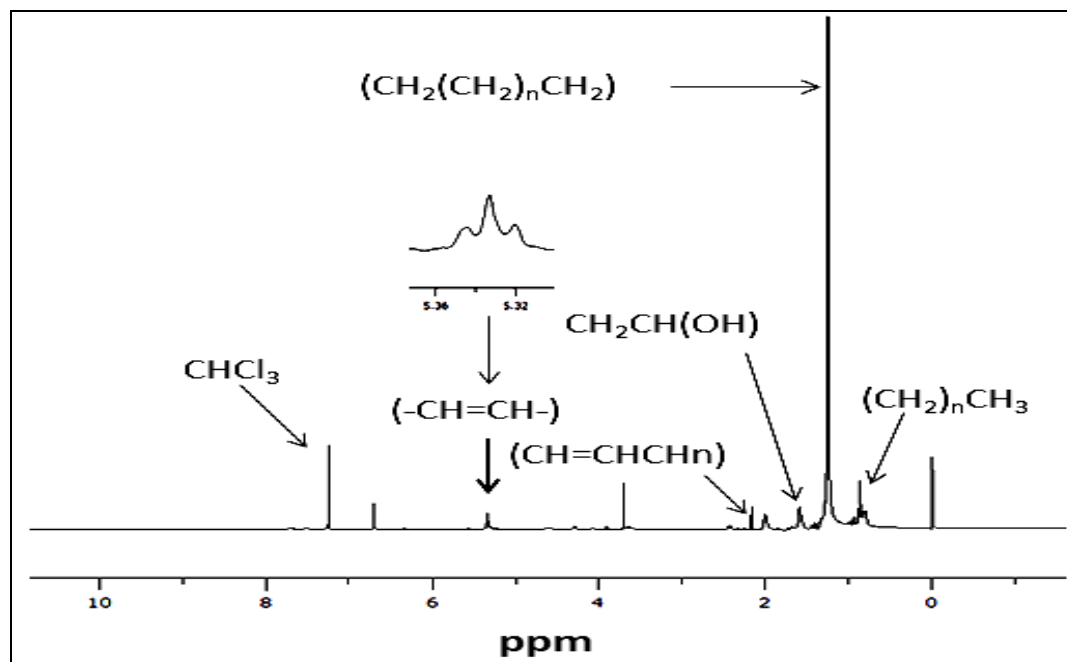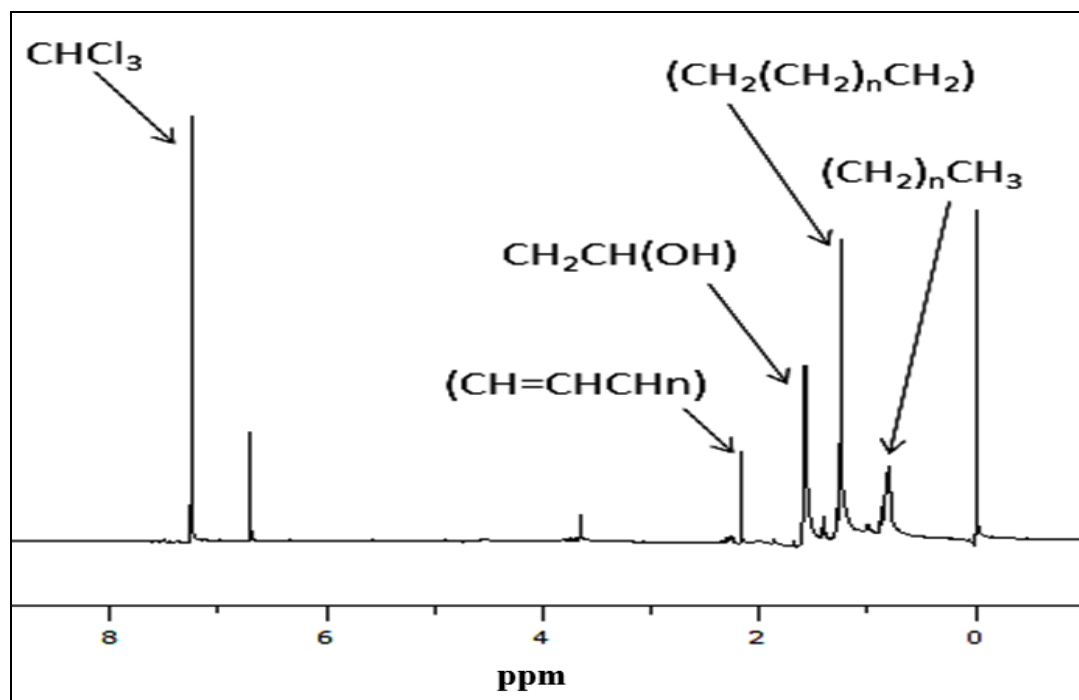
Figure 5.14: ^{1}NMR spectra of the α mycolic acid of [A] Wild type, mc^{2}155 and [B] *eccD3* mutant, Ms0622.

The spectra of the epoxy component of the mycolic acid methyl ester isolated from both the wild type (mc^{2}155) and the *eccD3* deleted strain (Ms0622) was compared. From the comparison it was observed that the signal attributed by the protons adjacent to the *cis* double bond at δ (ppm)=2.02 and δ (ppm)=5.35 the wild-type (Figure 5.15 [A]) was absent in the *eccD3* deleted strain (Figure 5.15 [B]). Moreover, the shift observed at δ (ppm)=4.5 characteristic of the proton of the hydroxyl group in the parental strain was more intense as compared to the *eccD3* deleted strain. This confirmed the absence of the oxirane group in the epoxy component
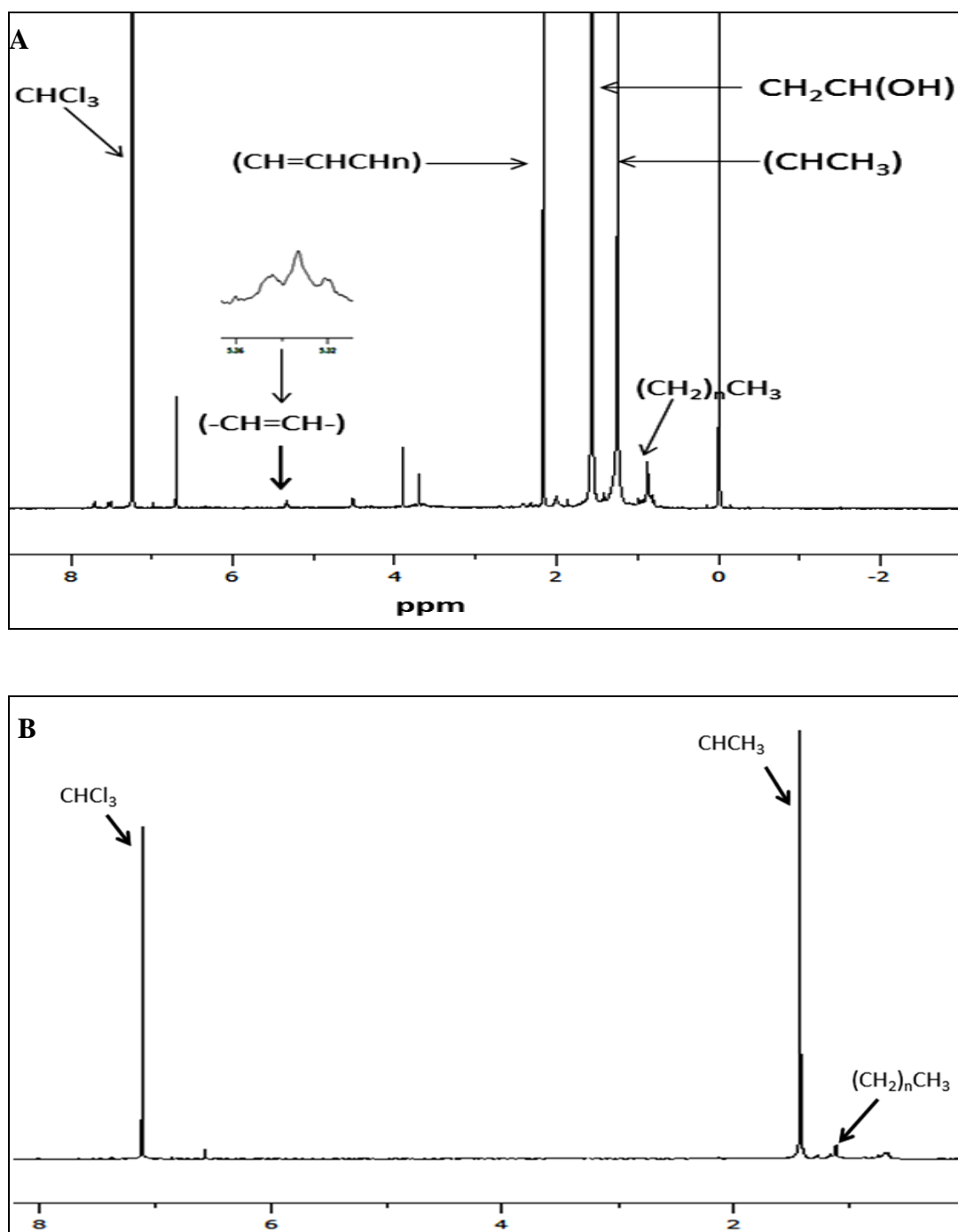
Figure 5.15: ¹H NMR spectra of 'epoxy' subspecies of Mycolic acid methyl esters extracted from [A] Wild type, mc²155 and [B] *eccD3* deleted mutant, Ms0622

5.4   Discussion

Unlike the Gram positive and Gram negative bacteria, species belonging to mycobacteria have a very unique cell wall with a thick mycomembrane outer layer

which contributes to the basic physiological and pathogenic features of the bacterium and at the same time serves as the most susceptible and resistant impediment to many anti tuberculosis drugs [46,47]. The cell envelope of *Mycobacterium* comprises of three parts-(i) the outermost layer; (ii) the cell wall; and (iii) the plasma membrane of which the cell wall is a complex of mycomembrane (MM), arabinogalactan (AG) and peptidoglycan (PG) [48]. The mycomembrane is organized in a non-conventional lipid bilayer arrangement in which the mycolic acids are esterified to the arabinogalactan layer and the latter is surrounded by the peptidoglycan layer [10,48,49]. This outer mycomembrane hosts the porin proteins through which the transfer of the hydrophilic molecules occur across the mycobacterial membrane and also certain secretory machineries which secrete the virulence factors *viz*., the ESAT6 and the CFP10 proteins [50-53]. The presence of the secretory apparatuses such as the T7SS in the outer mycomembrane of the *Mycobacterium* suggests the possible role of these secretion apparatuses in the precise organization of the mycobacterial cell wall architecture. In a study by Bottai *et al*, 2012, demonstrated the role of T7SS associated ESX-5 in maintaining the cell wall integrity of the mycobacterial cell wall [54]. In this chapter the role of the ESX-3 associated *eccD3* gene in preserving the precise architecture of the *M. smegmatis* cell wall has been demonstrated.

The study demonstrates the role of ESX3 associated *eccD3* gene in maintaining the shape of the mycobacterial cells. The deletion of the *eccD3* gene resulted in the irregular shape of the bacteria. The shape of the bacteria is a very important aspect as it directly influences its ability to acquire nutrients from its surrounding environment, motility, the ability for the proper partitioning of the genetic material and localization of the secretion apparatuses. The shape of a bacterium is determined by the complex mesh of the peptidoglycan that surrounds the bacteria which in turn are produced as a result of many enzymatic pathways. These enzymes organize into complexes and thereby determine the shape of the bacterium [1,55]. Several works have demonstrated the resulting appearance of the colony and cell morphology has a direct relationship with the cell wall structure of the bacterium. Meniche *et al,* 2014 studied the dynamics of cell wall synthesis and its relation in maintaining the cellular morphology of the bacterium. They showed synthesis of the 2-carboxyacyl-CoA (C_{22}–C_{26}) mycolate precursor occurs at the pole tip and the synthetic enzymes control the elongation rate in mycobacteria [56-58]. A similar defect in the cell morphology was observed in a CrgA deleted *M. smegmatis* mutant

which was reported to interact with the cell wall synthesis machinery [59]. A strong correlation exists between the cell wall synthesis machinery and the shape of the bacterium. This was evident from the studies by Plocinski *et al*, 2011 in which they reported the involvement of Wag31 and Cws in the synthesis of the cell wall and thereby its influence in the maintenance of the mycobacterial cell shapes [60]. Similar to this report, deletion of the mycolic acid methyltransferases (MAMTs) resulted in mycolic acid which eventually leads to small, smooth and doughnut-shaped colony formation [61].

In the previous chapter, the possible role of the *eccD3* gene in the precise organization of the cell wall was demonstrated which was evident from the abnormal colony morphology of the *eccD3* knockout mutant strain, its inability to form biofilm and decrease in the cell wall permeability. In concordance with the earlier results, it is found in the current study that the *eccD3* deleted mutant strain lacked mycolic acid. The mycolic acids extracted from the parental strain and the *eccD3* deleted *M. smegmatis* strain, Ms0622 were separated on a TLC plate. The mycolic acid extracted from the wild-type *M. smegmatis* was resolved into three distinct components-α, α′ and epoxy mycolic acid methyl esters but the mycolic acid methyl ester extracted from *eccD3* deleted strain, Ms0622 exhibited only the α-component of mycolic acid. The α-subspecies of the methylated mycolic acid esters extracted from mutant strain was present only in traceable amounts. The *eccD3* deleted strain also lacked the α′ and epoxy subspecies of mycolic acid methyl esters. The synthesis of mycolic acid comprises of the two FASI and FASII system in which the short chain length and the long chain length fatty acids are synthesized respectively. A large number of enzymes are involved in the sequential synthesis of these fatty acids in the bacterium. It is important to note that during the division of a mycobacterial cell, the cell wall has to be synthesized constitutively. However, the genetic determinants or the enzymes involved in the coordinated synthesis of the mycobacterial cell wall and the cell division are yet to be deciphered. In the rod shaped bacteria, MreB protein is involved in the synthesis of cell wall while the FtsZ tubulin like protein helps in the formation of the septasomal complex leading to the formation of septum in the dividing daughter cells [62,63]. The *Mycobacterium* species possesses the FtsZ homolog while its counterpart, MreB protein homolog is absent in the mycobacterial species [59,64]. In the present study, the conversion of the rod shaped bacilli to coccus shaped

cells in the *eccD3* deleted *M. smegmatis* strain, Ms0622 and the absence of the constituent α′ and epoxy mycolic acid methyl ester subspecies was observed which suggested the probable involvement of the ESX3 associated *eccD3* gene in the coordinated synthesis machinery of cell wall synthesis and determination of the cell shape structure.

The unique architecture of the mycobacterial cell wall composed of lipid bilayer to which the mycolic acids are perpendicularly attached represents a sturdy barrier between the mycobacterial cells and the extracellular environment. It protects the bacterium from any harmful compounds by providing minimum fluidity to the innermost part of the membrane. The low fluidity of the mycobacterial membrane can be accounted from the high melting temperature of the fatty acid, around 60°C, observed by DSC [65,66]. These mycolic acids play a critical role in maintaining the low permeability and low fluidity of the mycobacterial cell wall that accounts for the intrinsic resistance of mycobacteria to hydrophobic drugs [36,67]. In the present study, the purified mycolic acid methyl ester from the *eccD3* deleted mutant strain showed an increase in the thermal transition by about 7^oC in comparison to the wild-type. The increase in the thermal transition temperature suggested low fluidity of the mutant cell wall than the parental strain. In a similar study, cyclopropanation of the mycolic acid in the proximal position in *M. smegmatis* occured as a result of expression of the cyclopropane synthetase enzyme, which thereby resulted in the rise in transition temperature by 3^oC. This rise in temperature provided low permeability of the cell envelop as reflected by the less susceptibility to peroxidation [21]. Similarly, the over expression of the enzyme involved in the synthesis of methoxymycolate, *mmas-1* in *M. tuberculosis* resulted in the decrease in temperature by 7^oC leading to a more permeable cell wall evidential from the increased uptake of chenodeoxycholate [68]. In the study, the deletion of the *eccD3* gene of the ESX3 secretion system resulted in decrease in the membrane permeability as evident from the rise in the thermal transition and less accumulation of the representative hydrophilic and hydrophobic compounds in the *eccD3* deleted strain as described in the previous chapter.

There are two structural features of the cell wall that contributes to the increase in transition temperature- i) The overall length of the hydrocarbon chains in the mycolic acid and ii) the degree of unsaturation of the hydrocarbon tails, *cis*-to-

trans conversion and introduction of *cis* cyclopropane rings [36,69-71]. Thus it was presumptuous that deletion of the *eccD3* gene in *M. smegmatis* might have altered the length of hydrocarbon tails (number of carbon atoms) present in the mycolic acid or the mycolic acid might have undergone desaturation resulting in the decrease in membrane fluidity. In order to verify this, the purified subspecies of methylated mycolic acid esters isolated from both the parental and the *eccD3* deleted *M. smegmatis* strains were subjected to GC-MS analysis. According to the GC-MS analyses, the α subspecies of mycolic acid methyl ester of the wild-type had the two characteristic peaks corresponding to the α-unit ($C_nH_{2n-1}O_2$, C=22, 26). The gas chromatogram of the α subspecies of mycolic acid methyl ester of the *eccD3* deleted strain, Ms0622 lacked the two characteristic peaks corresponding to the α-unit ($C_nH_{2n-1}O_2$, C=22, 26), instead it consisted of a peak corresponding to a α-unit with less number carbon atoms (C_{18}). Moreover, odd number carbon atoms in the α component was absent in the mutant strain. Since the α′ and epoxy components were nearly absent, the results of GC-MS could not be analyzed. It was observed that the characteristic peaks of the Fatty acid methyl ester in the wild- type were also present in the *eccD3* knockout *M. smegmatis*. The synthesis of nascent mycolic acid chain involves several enzymes of which a protein, KasA plays a primary role in the nascent elongation of the fatty acid followed by the final elongation by the KasB enzyme [72]. In another study it was reported that deletion of the Kas A gene in *M. marinum* and *M. tuberculosis* resulted in the synthesis of mycolates that were shorter in length by two to six carbon atoms [73]. In the present study the role of the *eccD3* gene of the ESX3 T7SS in mycolate synthesis has been analysed. The α mycolic acid subspecies isolated from the *eccD3* deleted strain was shorter in length by four to six carbon atoms than the wild-type *M. smegmatis*. The formation of shorter length mycolic acids in the *eccD3* deleted strain was suggestive of the fact that the ESX3 T7SS is involved in the cell wall synthesis machinery of *M. smegmatis*.

When the mycolic acid subspecies isolated from both the parental and *eccD3* deleted *M. smegmatis* strains were subjected to ^{1}H NMR, it was observed that the two *cis* double bonds present in the α and epoxy subspecies of mycolic acid in the parental strain were converted to saturated carbon atoms in the *eccD3* deleted strains. The synthesis of the mature mycolic acid by the *Mycobacterium* takes the advantage of several multimeric enzymes. The entry of the FAS I system product to the FAS II

system involves the action of the β-ketoacyl-ACP- synthase III (mtFabH) [74,75]. However, the addition of the *cis* double bonds to the newly condensed mycolic acid is still not known. It is believed that β-hydroxyacyl-ACP dehydrase and 2-*trans*-enoyl-ACP isomerase might play a role in the addition of the *cis* double bond [15]. The proteins EchA10 and EchA11 present in *M. tuberculosis* homologous to the hydratase and invertase respectively of *E. coli* are believed to introduce the *cis* double bond in the distal meromycolate chain [15]. In another report it was demonstrated that the homologs of desaturase *viz.*, desA1, desA2 and desA3 in *M. tuberculosis* was involved in the synthesis of oleic and palmitic acid ($C_{16:1}\Delta9$), which later resulted in the formation of two *cis* double bonds [64,76]. Later, it was reported that the length of the precursor fatty acid determined the position of the *cis* double bond in mycolic acid and during the final step of condensation between the fatty acid and the meromycolic chain the *cis* double bonds were formed.

The resultant shorter length of the α- subspecies of mycolic acid methyl ester in the *eccD3* deleted strain and its subsequent saturation of the α and the epoxy subspecies have a major impact on the architecture of the cell wall resulting in the disintegration of the cell wall. The formation of the resultant saturated α and epoxy mycolic acid methyl esters in the *eccD3* deleted *M. smegmatis* strain provides an essence that the ESX3 T7SS might be involved in the elongation pathway of the mycolic acid as well as in the biosynthesis of the *cis-cis* diunsaturated mero acids.

The development of anti-tuberculosis drugs depends on the discovery and identification of potent targets upon inhibition of which might cure TB even in the latent stage. The biosynthetic pathway for cell wall synthesis has always been a potential target for anti-tuberculosis drug discovery. The length and high degree of unsaturation in the mycolic acid contributes to the less fluidity of the cell wall of *Mycobacterium* which in turn aids the bacteria to prevent any obnoxious compound in entering the cell thereby withstand any unfavorable condition presented by the host environment. The contribution of the ESX3 associated *eccD3* gene in maintaining the correct architecture of the cell wall and imparting the most important trait of low permeability of the mycobacterial cell wall presents itself as a most potent drug target. Moreover this study reinforces the use of *M. smegmatis* as a surrogate model for the study of Mycobacterial pathogenesis. Thus this study indicates a direct relationship between the cell wall structure and the ESX3 secretion system in *M.smegmatis*.

Reference List

[1]   Young, K.D. The selective value of bacterial shape. *Microbiology and molecular biology reviews*, 70(3):660-703, 2006.

[2]   Hett, E.C. and Rubin, E.J. Bacterial growth and cell division: a mycobacterial perspective. *Microbiology and Molecular Biology Reviews*, 72(1):126-156, 2008.

[3]   Scheffers, D.J. and Pinho, M.G. Bacterial cell wall synthesis: new insights from localization studies. *Microbiology and Molecular Biology Reviews*, 69:585-607, 2005.

[4]   Brennan, P.J. and Nikaido, H. The envelope of mycobacteria. *Annual review of biochemistry*, 64(1):29-63, 1995.

[5]   Ratledge,C., Stanford,J. The Biology of the mycobacteria Academic Press. eds., 1982.

[6]   Kang, C.M., Nyayapathy, S., Lee, J.Y., Suh, J.W., and Husson, R.N. Wag31, a homologue of the cell division protein DivIVA, regulates growth, morphology and polar cell wall synthesis in mycobacteria. *Microbiology,* 154:725-735, 2008.

[7]   Shaevitz, J.W. and Gitai, Z. The structure and function of bacterial actin homologs. *Cold Spring Harbor perspectives in biology*, 14:000364, 2010.

[8]   Van Teeffelen, S., Wang, S., Furchtgott, L., Huang, K.C., Wingreen, N.S., Shaevitz, J.W. and Gitai, Z. The bacterial actin MreB rotates, and rotation depends on cell-wall assembly. *Proceedings of the National Academy of Sciences*, 108(38):15822-15827, 2011.

[9]   Hett, E.C., Chao, M.C., Deng, L.L., and Rubin, E.J. A mycobacterial enzyme essential for cell division synergizes with resuscitation-promoting factor. *PLoS pathogens*, 4(2):e1000001, 2008.

[10]   Daffé, M. and Draper, P. The envelope layers of mycobacteria with reference to their pathogenicity. *In Advances in microbial physiology*, 39:131-203, Academic Press, 1997.

[11]   Brennan, P.J. and Goren, M.B. Structural studies on the type-specific antigens and lipids of the mycobacterium avium. Mycobacterium intracellulare.

Mycobacterium scrofulaceum serocomplex. Mycobacterium intracellulare serotype 9. *Journal of Biological Chemistry*, 254(10):4205-4211, 1979.

[12]   Jarlier, V.I.N.C.E.N.T. and Nikaido, H.I.R.O.S.H.I. Permeability barrier to hydrophilic solutes in Mycobacterium chelonei. *Journal of bacteriology*, 172(3):1418-1423, 1990.

[13]   Hoffmann, C., Leis, A., Niederweis, M., Plitzko, J.M. and Engelhardt, H. Disclosure of the mycobacterial outer membrane: cryo-electron tomography and vitreous sections reveal the lipid bilayer structure. *Proceedings of the National Academy of Sciences*, 105(10):3963-3967, 2008.

[14]   Bloch, K. Control mechanisms for fatty acid synthesis in Mycobacterium smegmatis. *Advances in enzymology and related areas of molecular biology*, 45:1-84, 1977.

[15]   Takayama, K., Wang, C. and Besra, G.S. Pathway to synthesis and processing of mycolic acids in Mycobacterium tuberculosis. *Clinical microbiology reviews*, 18(1):81-101, 2005.

[16]   Laval, F., Lanéelle, M.A., Déon, C., Monsarrat, B. and Daffé, M. Accurate molecular mass determination of mycolic acids by MALDI-TOF mass spectrometry. *Analytical chemistry*, 73(18):4537-4544, 2001.

[17]   Dubnau, E., Lanéelle, M.A., Soares, S., Bénichou, A., Vaz, T., Promé, D., Promé, J.C., Daffé, M. and Quémard, A.K. Mycobacterium bovis BCG genes involved in the biosynthesis of cyclopropyl keto-and hydroxy-mycolic acids. *Molecular microbiology*, 23(2):313-322, 1997.

[18]   Baba, T., Kaneda, K., Kusunose, E., Kusunose, M., and Yano, I. Molecular species of mycolic acid subclasses in eight strains of Mycobacterium smegmatis. *Lipids*, 23(12):1132-1138, 1988.

[19]   Glickman, M.S., Cox, J.S. and Jacobs Jr, W.R. A novel mycolic acid cyclopropane synthetase is required for cording, persistence, and virulence of Mycobacterium tuberculosis. *Molecular cell*, 5(4):717-727, 2000.

[20]   Dubnau, E., Chan, J., Raynaud, C., Mohan, V.P., Lanéelle, M.A., Yu, K., Quémard, A., Smith, I. and Daffé, M. Oxygenated mycolic acids are necessary for virulence of Mycobacterium tuberculosis in mice. *Molecular microbiology*, 36(3):630-637, 2000.

[21]   George, K.M., Yuan, Y., Sherman, D.R. and Barry, C.E. The biosynthesis of cyclopropanated mycolic acids in Mycobacterium tuberculosis Identification

and functional analysis of CMAS-2. *Journal of Biological Chemistry*, 270(45):27292-27298, 1995.

[22] Daffe, M., Laneelle, M.A., Asselineau, C., Levy-Frebault, V. and David, H. Taxonomic value of mycobacterial fatty acids: proposal for a method of analysis. *In Annales de microbiologie*, 134(2):241-256, 1983.

[23] Watanabe, M., Aoyagi, Y., Ridell, M. and Minnikin, D.E. Separation and characterization of individual mycolic acids in representative mycobacteria. *Microbiology*, 147(7):1825-1837, 2001.

[24] Stanley, S.A., Raghavan, S., Hwang, W.W. and Cox, J.S. Acute infection and macrophage subversion by Mycobacterium tuberculosis require a specialized secretion system. *Proceedings of the National Academy of Sciences*, 100(22):13001-13006, 2003.

[25] van Pittius, N.C.G., Gamieldien, J., Hide, W., Brown, G.D., Siezen, R.J. and Beyers, A.D. The ESAT-6 gene cluster of Mycobacterium tuberculosis and other high G+ C Gram-positive bacteria. *Genome biology*, 2(10):research0044-1, 2001.

[26] Serafini, A., Boldrin, F., Palù, G. and Manganelli, R. Characterization of a Mycobacterium tuberculosis ESX-3 conditional mutant: essentiality and rescue by iron and zinc. *Journal of bacteriology*, 191(20):6340-6344, 2009.

[27] Siegrist, M.S., Unnikrishnan, M., McConnell, M.J., Borowsky, M., Cheng, T.Y., Siddiqi, N., Fortune, S.M., Moody, D.B. and Rubin, E.J. Mycobacterial Esx-3 is required for mycobactin-mediated iron acquisition. *Proceedings of the National Academy of Sciences*, pnas-0900589106, 2009.

[28] Yenugu, S., Hamil, K.G., Radhakrishnan, Y., French, F.S., and Hall, S.H. The androgen-regulated epididymal sperm-binding protein, human beta-defensin 118 (DEFB118) (formerly ESC42), is an antimicrobial beta-defensin. *Endocrinology*, 145: 3165-3173, 2004.

[29] Alahari, A., Trivelli, X., Guerardel, Y., Dover, L.G., Besra, G.S., Sacchettini, J.C., Reynolds, R.C., Coxon, G.D., and Kremer, L. Thiacetazone, an antitubercular drug that inhibits cyclopropanation of cell wall mycolic acids in mycobacteria. *PLoS.One*. 2: e1343, 2007.

[30] Kaneda, K., Imaizumi, S. and Yano, I. Distribution of C22-, C24-and C26-α-unit-containing mycolic acid homologues in mycobacteria. *Microbiology and immunology*, 39(8):563-570, 1995.

[31] Laval, F., Haites, R., Movahedzadeh, F., Lemassu, A., Wong, C.Y., Stoker, N., Billman-Jacob, H. and Daffé, M. Investigating the function of the putative mycolic-acid methyltransferase UmaA: divergence between the Mycobacterium smegmatis and Mycobacterium tuberculosis proteins. *Journal of Biological Chemistry*. 2007.

[32] Hett, E.C., Chao, M.C., and Rubin, E.J. Interaction and modulation of two antagonistic cell wall enzymes of mycobacteria. *PLoS Pathogen*, 6: e1001020, 2010.

[33] Barry, C.E., Lee, R.E., Mdluli, K., Sampson, A.E., Schroeder, B.G., Slayden, R.A. and Yuan, Y. Mycolic acids: structure, biosynthesis and physiological functions. *Progress in lipid research*, 37(2):143-179, 1998.

[34] Patru, M.M. and Pavelka, M.S. A role for the class A penicillin-binding protein PonA2 in the survival of Mycobacterium smegmatis under conditions of nonreplication. *Journal of bacteriology*, 192(12):3043-3054, 2010.

[35] Dobson G., Minnikin D.E., Minnikin S.M., Parlett M., Goodfellow M., Ridell M., Magnusson M. Systematic analysis of complex mycobacterial lipids. In: Goodfellow M., Minnikin D.E., editors. Chemical Methods in Bacterial Systematics. Academic Press; London: 237–265, 1985.

[36] Purwantini, E. and Mukhopadhyay, B. Rv0132c of Mycobacterium tuberculosis encodes a coenzyme F420-dependent hydroxymycolic acid dehydrogenase. *PLoS.One*, 8(12):e81985, 2013.

[37] Liu, J., Barry, C.E., Besra, G.S. and Nikaido, H. Mycolic acid structure determines the fluidity of the mycobacterial cell wall. *Journal of Biological Chemistry*, 271(47):29545-29551, 1996.

[38] Asselineau, J. and Lederer, E. Structure of the mycolic acids of mycobacteria. *Nature*, 166(4227):782, 1950.

[39] Baba, T., Kaneda, K., Kusunose, E., Kusunose, M. and Yano, I. Molecular species of mycolic acid subclasses in eight strains of Mycobacterium smegmatis. *Lipids*, 23(12):1132-1138, 1988.

[40]   Kaneda, K., Naito, S., Imaizumi, S., Yano, I., Mizuno, S., Tomiyasu, I., Baba, T., Kusunose, E. and Kusunose, M. Determination of molecular species composition of C80 or longer-chain alpha-mycolic acids in Mycobacterium spp. by gas chromatography-mass spectrometry and mass chromatography. *Journal of clinical microbiology*, 24(6):1060-1070, 1986.

[41]   Kusaka, T. and Mori, T. Pyrolysis gas chromatography-mass spectrometry of mycobacterial mycolic acid methyl esters and its application to the identification of Mycobacterium leprae. *Microbiology*, 132(12):3403-3406, 1986.

[42]   Yano, I., Kageyama, K., Ohno, Y., Masui, M., Kusunose, E., Kusunose, M. and Akimori, N. Separation and analysis of molecular species of mycolic acids in Nocardia and related taxa by gas chromatography mass spectrometry. *Biological Mass Spectrometry*, 5(1):14-24, 1978.

[43]   TOMIYASU, I. and YANO, I. Separation and analysis of novel polyunsaturated mycolic acids from a psychrophilic, acid-fast bacterium, Gordona aurantiaca. *The FEBS Journal*, 139(1):173-180, 1984.

[44]   Kaneda, K., Imaizumi, S., Mizuno, S., Baba, T., Tsukamura, M. and Yano, I. Structure and molecular species composition of three homologous series of α-mycolic acids from Mycobacterium spp. *Microbiology*, 134(8):2213-2229, 1988.

[45]   Yuan, Y. and Barry, C.E. A common mechanism for the biosynthesis of methoxy and cyclopropyl mycolic acids in Mycobacterium tuberculosis. *Proceedings of the National Academy of Sciences*, 93(23):12828-12833, 1996.

[46]   Wong, M.Y., Steck, P.A. and Gray, G.R. The major mycolic acids of Mycobacterium smegmatis. Characterization of their homologous series. *Journal of Biological Chemistry*, 254(13):5734-5740, 1979.

[47]   Barry, C.E., Crick, D.C. and McNeil, M.R. Targeting the formation of the cell wall core of M. tuberculosis. *Infectious Disorders-Drug Targets* (*Formerly Current Drug Targets-Infectious Disorders*), 7(2):182-202, 2007.

[48]   Jackson, M., McNeil, M.R. and Brennan, P.J. Progress in targeting cell envelope biogenesis in Mycobacterium tuberculosis. *Future microbiology*, 8(7):855-875, 2013.

[49]   Dafé, M., Quémard, A. & Marrakchi, H. Mycolic Acids: From Chemistry to Biology. Biogenesis of Fatty Acids, *Lipids and Membranes* in press (ed.,

Geiger, O.) Springer International Publishing, doi:https://doi.org/10.1007/978-3-319-43676-0_18-1, 2017.

[50]   Marrakchi, H., Lanéelle, M.A. and Daffé, M. Mycolic acids: structures, biosynthesis, and beyond. *Chemistry & biology*, 21(1):67-85, 2014.

[51]   Stahl, C., Kubetzko, S., Kaps, I., Seeber, S., Engelhardt, H. and Niederweis, M. MspA provides the main hydrophilic pathway through the cell wall of Mycobacterium smegmatis. *Molecular microbiology*, 40(2):451-464, 2001.

[52]   Harboe, M., Oettinger, T., Wiker, H.G., Rosenkrands, I. and Andersen, P. Evidence for occurrence of the ESAT-6 protein in Mycobacterium tuberculosis and virulent Mycobacterium bovis and for its absence in Mycobacterium bovis BCG. *Infection and immunity*, 64(1):16-22, 1996.

[53]   Buddle, B.M., Parlane, N.A., Keen, D.L., Aldwell, F.E., Pollock, J.M., Lightbody, K. and Andersen, P. Differentiation between Mycobacterium bovis BCG-vaccinated and M. bovis-infected cattle by using recombinant mycobacterial antigens. *Clinical and diagnostic laboratory immunology*, 6(1):1-5, 1999.

[54]   Moradi, J., Mosavari, N., Ebrahimi, M., Arefpajohi, R. and Tebianian, M. Evaluation of Mycobacterium tuberculosis early secreted antigenic target 6 recombinant protein as a diagnostic marker in skin test. *Osong public health and research perspectives*, 6(1):34-38, 2015.

[55]   Bottai, D., Di Luca, M., Majlessi, L., Frigui, W., Simeone, R., Sayes, F., Bitter, W., Brennan, M.J., Leclerc, C., Batoni, G. and Campa, M. Disruption of the ESX-5 system of Mycobacterium tuberculosis causes loss of PPE protein secretion, reduction of cell wall integrity and strong attenuation. *Molecular microbiology*, 83(6):1195-1209, 2012.

[56]   Huang, K.C., Mukhopadhyay, R., Wen, B., Gitai, Z. and Wingreen, N.S. Cell shape and cell-wall organization in Gram-negative bacteria. *Proceedings of the National Academy of Sciences*, 105(49):19282-19287, 2008.

[57]   Meniche, X., Otten, R., Siegrist, M.S., Baer, C.E., Murphy, K.C., Bertozzi, C.R. and Sassetti, C.M. Subpolar addition of new cell wall is directed by DivIVA in mycobacteria. *Proceedings of the National Academy of Sciences*, 111(31):E3243-E3251, 2014.

[58]   Kang, C.M., Abbott, D.W., Park, S.T., Dascher, C.C., Cantley, L.C. and Husson, R.N. The Mycobacterium tuberculosis serine/threonine kinases PknA

and PknB: substrate identification and regulation of cell shape. *Genes & development*, 19(14):1692-1704, 2005.

[59] Gande, R., Dover, L.G., Krumbach, K., Besra, G.S., Sahm, H., Oikawa, T. and Eggeling, L. The two carboxylases of Corynebacterium glutamicum essential for fatty acid and mycolic acid synthesis. *Journal of bacteriology*, 189(14):5257-5264, 2007.

[60] Plocinski, P., Ziolkiewicz, M., Kiran, M., Vadrevu, S.I., Nguyen, H.B., Hugonnet, J., Veckerle, C., Arthur, M., Dziadek, J., Cross, T.A. and Madiraju, M., Characterization of CrgA, a new partner of the Mycobacterium tuberculosis peptidoglycan polymerization complexes. *Journal of bacteriology*, JB-00188, 2011.

[61] Plocinski, P., Arora, N., Sarva, K., Blaszczyk, E., Qin, H., Das, N., Plocinska, R., Ziolkiewicz, M., Dziadek, J., Kiran, M., Gorla, P., Cross, T.A., Madiraju, M., and Rajagopalan, M. Mycobacterium tuberculosis CwsA interacts with CrgA and Wag31, and the CrgA-CwsA complex is involved in peptidoglycan synthesis and cell shape determination. *Journal of bacteriology*, 194: 6398-6409, 2012.

[62] Barkan, D., Hedhli, D., Yan, H.G., Huygen, K. and Glickman, M.S. Mycobacterium tuberculosis lacking all mycolic acid cyclopropanation is viable but highly attenuated and hyperinflammatory in mice. *Infection and immunity*, 80(6):1958-1968, 2012.

[63] Adams, D.W. and Errington, J. Bacterial cell division: assembly, maintenance and disassembly of the Z ring. *Nature Reviews Microbiology*, 7(9):642, 2009.

[64] White, C.L. and Gober, J.W. MreB: pilot or passenger of cell wall synthesis?. *Trends in microbiology*, 20(2):74-79, 2012.

[65] Cole, S., Brosch, R., Parkhill, J., Garnier, T., Churcher, C., Harris, D., Gordon, S.V., Eiglmeier, K., Gas, S., Barry Iii, C.E. and Tekaia, F. Deciphering the biology of Mycobacterium tuberculosis from the complete genome sequence. *Nature*, 393:537–544. 1998.

[66] Nikaido, H., Kim, S.H. and Rosenberg, E.Y. Physical organization of lipids in the cell wall of Mycobacterium chelonae. *Molecular microbiology*, 8(6):1025-1030, 1993.

[67] Liu, J.U.N., Rosenberg, E.Y. and Nikaido, H. Fluidity of the lipid domain of cell wall from Mycobacterium chelonae. *Proceedings of the National Academy of Sciences*, 92(24):11254-11258, 1995.

[68] Wang, L., Slayden, R.A., Barry, C.E. and Liu, J. Cell wall structure of a mutant of Mycobacterium smegmatis defective in the biosynthesis of mycolic acids. *Journal of Biological Chemistry*, 275(10):7224-7229, 2000.

[69] Yuan, Y., Crane, D.C., Musser, J.M., Sreevatsan, S. and Barry, C.E. MMAS-1, the branch point between *cis*-and *trans*-cyclopropane-containing oxygenated mycolates in Mycobacterium tuberculosis. *Journal of Biological Chemistry*, 272(15):10041-10049, 1997.

[70] Tomiyasu, I., Mycolic acid composition and thermally adaptative changes in Nocardia asteroides. *Journal of bacteriology*, 151(2):828-837, 1982.

[71] Tomiyasu, I., Toriyama, S., Yano, I. and Masui, M. Changes in molecular species composition of nocardomycolic acids in Nocardia rubra by the growth temperature. *Chemistry and Physics of Lipids*, 28(1):41-54, 1981.

[72] Baba, T., Kaneda, K., Kusunose, E., Kusunose, M. and Yano, I. Thermally adaptive changes of mycolic acids in Mycobacterium smegmatis. *The Journal of Biochemistry*, 106(1):81-86, 1989.

[73] Barry, C.E., Lee, R.E., Mdluli, K., Sampson, A.E., Schroeder, B.G., Slayden, R.A. and Yuan, Y. Mycolic acids: structure, biosynthesis and physiological functions. *Progress in lipid research*, 37(2):143-179, 1998.

[74] Gao, L.Y., Laval, F., Lawson, E.H., Groger, R.K., Woodruff, A., Morisaki, J.H., Cox, J.S., Daffe, M. and Brown, E.J. Requirement for kasB in Mycobacterium mycolic acid biosynthesis, cell wall impermeability and intracellular survival: implications for therapy. *Molecular microbiology*, 49(6):1547-1563, 2003.

[75] Choi, K.H., Kremer, L., Besra, G.S. and Rock, C.O. Identification and substrate specificity of β-ketoacyl (acyl carrier protein) synthase III (mtFabH) from Mycobacterium tuberculosis. *Journal of Biological Chemistry*, 275(36):28201-28207, 2000.

[76] Scardale, J. N., G. Kazanina, X. He, K. A. Reynolds, and H. T. Wright. Crystal structure of the Mycobacterium tuberculosis β-ketoacyl-acyl carrier protein synthase III. *Journal of Biological Chemistry*, 276:20516–20522, 2001.

[77]   Phetsuksiri, B., M. Jackson, H. Scherman, M. McNeil, G. S. Besra, A. R. Baulard, R. A. Slayden, A. E. DeBarber, C. E. Barry III, M. S. Baird, D. C. Crick, and P. J. Brennan. Unique mechanism of action of the thiourea drug isoxyl on Mycobacterium tuberculosis. *Journal of Biological Chemistry*, 278:53123–53130, 2003.